Geobarrier System for Protection Against Rainfall-induced Slope Failure

Harianto Rahardjo, *Professor, School of Civil and Environmental Engineering, Nanyang Technological University, Singapore; email: chrahardjo@ntu.edu.sg*
Alfrendo Satyanaga, *Senior Research Fellow, School of Civil and Environmental Engineering, Nanyang Technological University, Singapore, email: alfrendo@ntu.edu.sg*
Nurly Gofar, *Associate Professor, Postgraduate Program Universitas Bina Darma, Jl. Jendral Ahmad Yani, Palembang, Indonesia and Former Research Fellow, School of Civil and Environmental Engineering, Nanyang Technological University, Singapore, email: nurly_gofar@binadarma.ac.id*
Eng Choon Leong, *Associate Professor, School of Civil and Environmental Engineering, Nanyang Technological University, Singapore, email: cecleong@ntu.edu.sg*
Jernice Huiling Kew, *Senior Engineer, Building Research Institute, Housing & Development Board, HDB Hub 480, Lorong 6, Toa Payoh, Singapore, email: Jernice_HL_KEW@hdb.gov.sg*
Chien Looi Wang, *Deputy Director, Infrastructure and Development Research, Building Research Institute, Housing & Development Board, HDB Hub 480, Lorong 6, Toa Payoh, Singapore, email: wcll@hdb.gov.sg*
Johnny Liang Heng Wong, *Group Director, Building Research Institute, Housing & Development Board, HDB Hub 480, Lorong 6, Toa Payoh, Singapore, email: Johnny_LH_Wong@hdb.gov.sg*

ABSTRACT: *Slope failures are a common occurrence in tropical regions with a high intensity of rainfall. Tropical areas such as Singapore are normally covered with residual soils whose behaviour does not follow the principles of classical saturated soil mechanics because these soils are often unsaturated in nature. The negative pore-water pressure in unsaturated soil is highly influenced by the changes in the flux boundary conditions, resulting from the variation in climatic conditions. On the other hand, the negative pore-water pressure contributes additional shear strength to the unsaturated soil. As water infiltrates into the slope, pore-water pressure in the slope increases (matric suction decreases), and the additional shear strength due to matric suction will decrease, causing the slope to be more susceptible to failure. Singapore is a land scarce country with a critical need to optimize land utilization. Steepening slopes or cutting back slopes and supporting them using a retaining structure is one way to create new spaces. In this study, a new type of retaining structure, Geobarrier System (GBS) is proposed. A GBS is a man-made three-layer cover system designed as a vegetative layer combined with a two-layer unsaturated system, which harnesses the distinct difference in unsaturated hydraulic properties between a fine-grained layer and a coarse-grained layer. GBS consists of recycled materials and does not use steel or concrete and is hence more cost effective, thereby making it economical for use in urban areas. Geobag for the vegetative layer is supported by specially designed pockets for planting different types of sustainable plant species. The paper presents the design, construction procedures, material selection and field performance of a GBS constructed at an inclination angle of 70^o in response to rainfall infiltration. In addition, the results of the finite element seepage and slope stability analyses of the GBS subjected to extreme rainfalls are also presented. The results from field instruments and numerical analyses showed that GBS was able to protect the slope from rainfall infiltration; therefore, the stability of the slope retained by GBS was not affected by the rainfall.*

KEYWORDS: Geobarrier system, Field instrumentation, Recycled concrete, Recycled asphalt.

SITE LOCATION: Geo-Database

INTRODUCTION

Slope failures in Singapore, which is mostly covered with residual soils, commonly occur due to high intensity of rainfall (Tsaparas et al., 2002; Rahardjo et al., 2011; 2012a). The residual soil is commonly observed in unsaturated zone above the groundwater table. Negative pore-water pressure or matric suction of the unsaturated soil contributes an additional shear strength as an apparent cohesion (Fredlund and Rahardjo, 1993). As water infiltrates into the slope, the pore-water pressure in the slope increases and the additional shear strength due to matric suction will decrease, causing the slope to be more susceptible to failure (Toll et al., 1999; Rahardjo et al., 2005, 2014a, b).

Methods to stabilize and protect slopes from rainfall infiltration have been developed by many researchers (Yan and Chu, 2008; Siah and Tseng, 2011; Wen et al., 2016; Rahardjo et al., 2012b). On the other hand, a good understanding of the mechanism leading to rainfall-induced slope failure is required for selecting a suitable preventive measure. Geosynthetics-reinforced soil structures have been used widely as stabilization method due to some of the advantages including ease of construction and the use of local soil as reinforced material (Koerner, 2005). The structure comprises three components i.e. reinforced soil fill, reinforcing element, and facing. Previous researches showed that drainage provisions should be provided to protect the structure from rainfall infiltration, raise of groundwater table and seepage from the back of reinforced zone (Koerner and Koerner, 2011) because the accumulation of water within the reinforced zone could increase the total force against the retaining structure significantly resulting in large wall deformation.

Capillary barrier has been developed as a slope protection to minimize rainwater infiltration into residual soil slopes in Singapore by Rahardjo et al (2007). The capillary barrier system utilizes the contrast in hydraulic properties of fine- and coarse-grained layers in unsaturated conditions to limit water percolation into the underlying soil layers (Tami et al., 2004; Rahardjo et al., 2016). The Zhan et al. (2014) study indicated that an inclined three-layer cover with capillary barrier effect (CCBE) comprising silt, sand, and gravel performed well in protecting a slope in Southern China under a humid climate and high intensity and long duration of rainfalls. Field monitoring (Rahardjo et al., 2010, 2012b, 2013, 2017) proved that the capillary barrier system was effective to minimize rainwater infiltration as well as maintain the stability of slope up to about 35^o inclination angle. However, the creation of new space is a growing concern in Singapore which leads to steepening slopes or cutting back slopes. The construction of a slope steeper than 35^o requires consideration of a retaining structure. Thus, a retaining structure that incorporates capillary barrier system is needed to mitigate rainfall-induced failures in steep slopes of tropical regions such as Singapore.

Based on the problems stated in the preceding discussion, Rahardjo et al (2015) developed the Geobarrier System (GBS), a retaining structure that incorporates capillary barrier system. The system consists of geobags that are made from geosynthetics and are filled with soils or granular materials (Matsuoka et al. 2001). In line with current sustainable environment policies, recycled materials such as recycled concrete aggregate (RCA) and reclaimed asphalt pavement (RAP) can be used to replace natural aggregates as components of the capillary barrier system (Rahardjo et al. 2013; McCulloch et al. 2017). In this case, the bags filled with fine-grained recycled materials (fine RCA or RAP) are placed on top of a layer of coarse-grained recycled materials (coarse RCA or RAP) as the components of a capillary barrier system. Rahardjo et al. (2018a) showed that the presence of bags between the fine- and coarse-grained materials did not interfere with the effectiveness of the capillary barrier system. Approved soil mixture (ASM) was also contained in bags and placed in front of the fine-grained layer to facilitate the planting of deep and widespread rooted shrubs/trees as part of wall facing.
The objective of this paper is to present a case study of a GBS system that was constructed at Orchard Boulevard, Singapore. The paper presents the overall design, and construction procedures of GBS for slope at Orchard Boulevard. Furthermore, the performance of the GBS in response to rainfall infiltration is discussed in the paper based on the field monitoring data and the results of the finite element seepage and slope stability analyses.

DESIGN AND CONSTRUCTION OF GEOBARRIER SYSTEM

Components of GBS

The GBS comprises three integrated functions: (1) retaining structure system, (2) capillary barrier system, and (3) green cover. The component materials for the specified function are shown in Table 1. The retaining structure system consists of

Submitted: 26 June 2018; Published: 16 August 2019
Reference: Rahardjo, H., Satvanaga, A., Gofar, N., Leong, E.C., Kew, J.H., Wang, C.L. and Wong, J.L.H. (2019). Geobarrier System for Protection Against Rainfall-induced Slope Failure. International Journal of Geoengineering Case Histories, Vol.5, Issue 1, p. 26 - 42. doi: 10.4417/IJGCH-05-01-03

compacted residual soil as reinforced fill, geogrids as reinforcing element, and combination of bags filled with recycled material and ASM as facing. The capillary barrier system is made of bags filled with fine-grained recycled material laid on top of a layer of coarse-grained recycled material. The green cover is vegetation planted in bags filled with ASM. The system was also enhanced with proper drainage system including gravel sump below the toe to collect the rainwater from the fine-grained layer and drain it out to the main drainage system as well as two rows of surface drain at the crest to collect run-off. The surface drainage is located at a suitable distance so that the reinforced soil will not be affected by seepage from behind the system. The schematic diagram of GBS is shown in Figure 1.

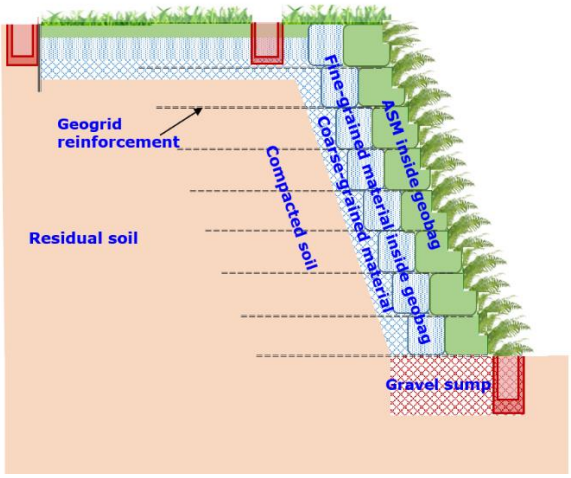


Figure 1. Schematic diagram of GBS.

Table 1. Components of GBS based on function.

	Fine-grained Material	Coarse-grained Material	Geobag
Capillary Barrier System	Recycled material RCA or RAP	Recycled material RCA or RAP	Woven Geotextile
	Facing Element	Reinforcing Element	Reinforced Fill
Retaining Structure (Reinforced Soil System)	Bags of Fine-grained material & ASM	Geogrids	Compacted Residual soil (in-situ)
Green Cover	Approved soil mix (ASM)	Specially designed Geobag	Specified Plants

Two sizes of material are used in GBS as the components of a capillary barrier system. The fine-grained material is wrapped in a geobag and stacked on top of each other on the slope face to form a retaining structure. The coarse-grained material is placed behind the bags of the fine-grained material to limit water infiltration into the compacted residual soil which also acts as a component of the reinforced retaining structure system. Since GBS incorporates green cover in the system, an approved soil mixture (ASM) was required for plants to grow adequately. The ASM is confined in a geotextile bag and placed in front of the bags of the fine-grained material. Geogrid is connected to the ASM bag and acts as reinforcement in the retaining structure system. Since the geogrids are connected to the ASM bag, then the ASM bags also plays a role of facing in the reinforced retaining structure system.

Two types of recycled materials, i.e. recycled concrete aggregate (RCA) and reclaimed asphalt pavement (RAP) with two different gradations, i.e. fine and coarse RCA and RAP were used as materials in GBS. The fine-grained layer was compacted

to relative density (D_r) between 70–90% or to the required dry density (ρ_d) between 1.62-1.67 Mg/m^3. The coarse-grained layer was compacted to relative density (Dr) between 70–90% or to the required dry density (ρ_d) between 1.53-1.57 Mg/m^3. Since GBS incorporated green cover in the system, approved soil mixture (ASM) was required for plants to grow adequately. GBS uses in-situ soil as reinforced fill. The soil should be compacted to 90% of the maximum dry density based on the Standard Proctor compaction curve. The soil should be compacted to 90% dry density based on laboratory compaction curve. The actual compaction level should be checked in-situ for each placement layer of soil using the sand cone test (ASTM D1556). Geotextile used in manufacturing the geobags is made of a woven monofilament fibre weaved to form a stable matrix with high water flow and optimum opening size for soil retention. The geotextile should have a tensile strength greater than or equal to 50 kN/m at 20% strain; puncture strength of greater than or equal to 5.0 kN; pore size (O_{90}) of less than or equal to 600 microns; and water permeability greater than or equal to 0.2 m/s.

Figure 2 shows the geobags used for fine-grained material and ASM. The dimension of ASM geobag is 0.6 m width × 0.5 m height × 1.5 m length while the dimension of the geobag for the fine-grained material is 0.5 m width × 0.5 m height × 1.5 m length. The ASM bag is supported by specially designed pockets for planting different types of plants. The ASM bag is also connected to geogrids used as a reinforcing element. The bi-axial geogrids should be made from high-quality polyester yarn fibres with high tensile strength with a design life of 120 years and a tensile strength of 12 kN/m @ 2% strain and 30 kN/m @ 5% strain.



Figure 2. Geotextile bags for fine material and ASM.

Construction Procedures

Construction of GBS was started with the excavation of the original slope to the required dimensions and depth of the GBS slope. A compacted gravel layer was placed at 1 m depth from the ground surface below the toe of the slope. The gravel layer was required near the slope toe in order to drain out the water from the GBS system into the main drain. During a rainfall event, some amount of water was expected to infiltrate into the ASM, the fine-grained and the coarse-grained layers before being discharged into the gravel sump at the base of the slope. Three corrugated perforated pipes were prepared to drain out water to the gravel sump, one from the coarse-grained layer, two from the fine-grained layer and one from the ASM layer. All pipes were wrapped with geotextile to avoid migration of soil particles that may block the pipe holes. The water from gravel sump was directed to the surface drain and then was channelled to the main drain. These stages are illustrated in Figure 3a.

The fine-grained material and the ASM were placed carefully into the geobags prior to the placement at the designated locations. The fine-grained material was compacted at a relative density between 70% and 90%. The placement of geobags was carried out in stages of 500 mm height. Each stage was started with the placement of the ASM geobag. The geogrid attached to ASM geobag was stretched up to its maximum length. Then, the geobag containing the fine-grained material was placed behind the ASM geobag. Residual soil was compacted to 90% compaction level to form a reinforced fill, leaving a 20 cm space between the compacted soil and the bag with the fine-grained material. Then, the coarse-grained material was placed and compacted to the required dry density. These steps are illustrated in Figure 3b and are repeated until the layer before the final level was reached (Figure 3c).

In the final stage of the GBS construction (at the crest of the slope), the coarse-grained material was placed directly above the ground surface behind the fine-grained material bag. Then, geofabric was placed on top of the coarse-grained material before the placement of the fine-grained material. Another geofabric layer was placed before laying ASM on top of the fine-grained material. Then, two surface drains were constructed at the specified locations. The crest of the GBS slopes were then covered by turfing on the ASM layer. These steps are illustrated in Figure 3d. Vegetations were planted in each pocket of the ASM geobags upon the completion of the GBS slopes. The diagram of the completed GBS is shown in Figure 1.

The performance of GBS was monitored by the installation of field instrumentation including rain gauge, piezometers, tensiometers, soil moisture sensors, water flow meter, and earth pressure sensor. Rainfall and groundwater level response to rainfall infiltration were monitored by rainfall gauge and piezometers installed at the crest and toe of the slope, respectively. Tensiometers and soil moisture sensors were used for the measurement of negative pore-water pressures and soil moisture changes due to rainwater infiltration. Water flow meters could be installed in the drains provided for water flow from the coarse-grained and fine-grained layers to check if there is any breakthrough into the coarse-grained layer during rainfall.

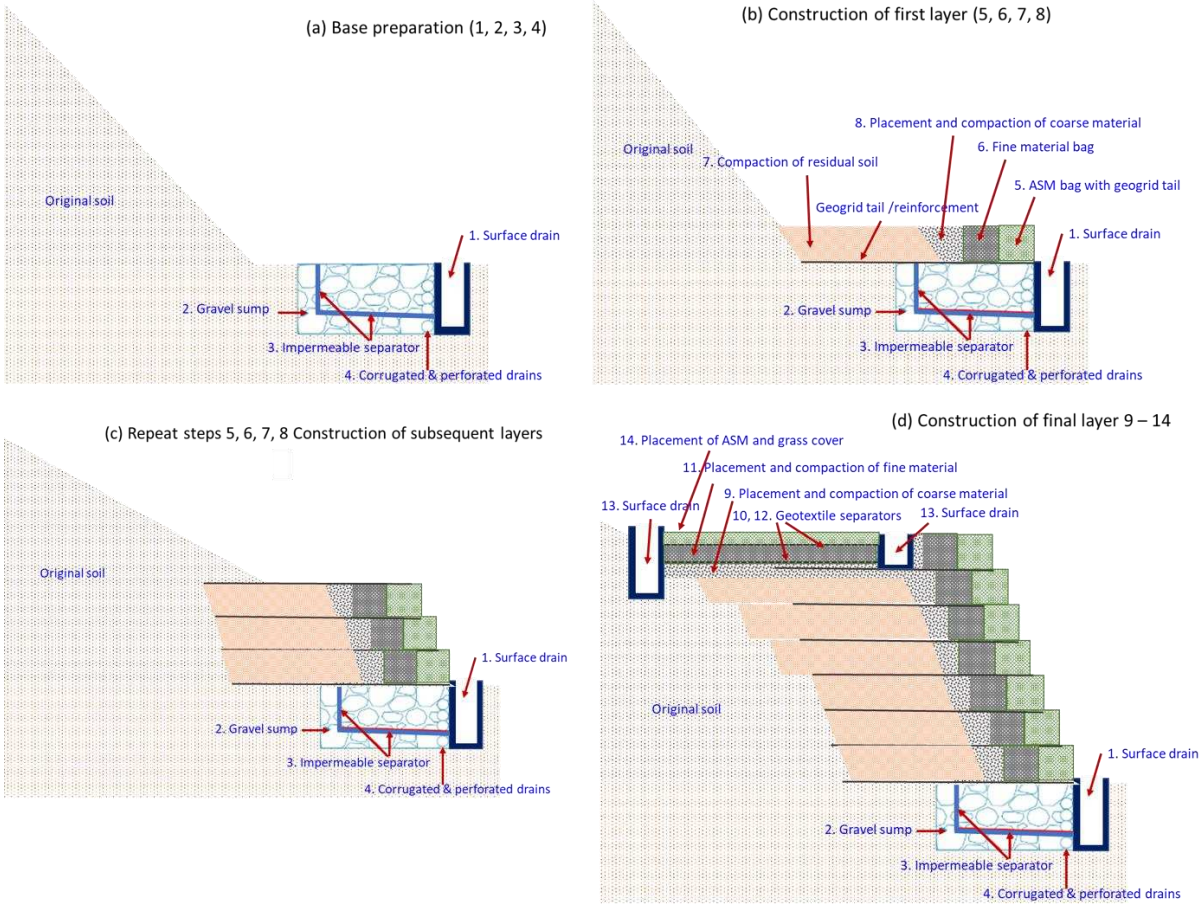


Figure 3. Construction stages of GBS.

CASE STUDY

GBS at Orchard Boulevard, Singapore

Three GBSs were constructed at Orchard Boulevard in Singapore with a slope height of 4 m and a slope angle of 70° (Figure 4). The original slope was inclined at 35°, thus the construction of the GBSs involved excavation of the slope to the designed slope angle. Preliminary site investigation indicated that the groundwater table was located at about 2 m and 6 m below the ground surface at the toe and crest, respectively. In other words, the residual soil below and behind the slope was in an unsaturated condition. The results from index properties for residual soil at Orchard Boulevard indicated that the residual soil

can be classified as moderate to high plasticity clay (CH) according to USCS with a total density of 1.80 Mg/m^3 and a dry density of 1.37 Mg/m^3. The residual soil consists of 20% sand, 27% silt and 53% clay.

GBS1 used fine and coarse RCA as the fine- and coarse-grained material, respectively. GBS2 used fine and coarse RAP as the fine- and coarse-grained material, respectively while GBS3 used fine RCA as the fine-grained material while coarse RAP was used as the coarse-grained material. As a retaining structure, the system comprises of three components i.e. facing, reinforcing element and reinforced fill. Geobags filled with fine RCA or fine RAP and bags of ASM serve as facing panel of the GBS. The reinforcement function was provided by geogrids while the reinforced fill was made of compacted residual soil available at the site. The in-situ soil was compacted to 90% relative density.
The presence of geobag at the interface between the fine- and coarse- grained materials did not interfere with the effectiveness of the capillary barrier system (Rahardjo et al. 2018a). The GBSs at Orchard Boulevard consisted of eight layers of geobags with a 2.8 m- long geogrids. The geogrids were secured in between two layers of geobags and connected to the ASM bags (Figure 2). A 0.3 m thick of coarse-grained material (coarse RCA or coarse RAP) was laid on the reinforced soil before the placement of bags of fine RCA or fine RAP (Figure 3). A cross-section of the GBSs at Orchard Boulevard is shown in Figure 5.



Figure 4. GBS at Orchard Boulevard.

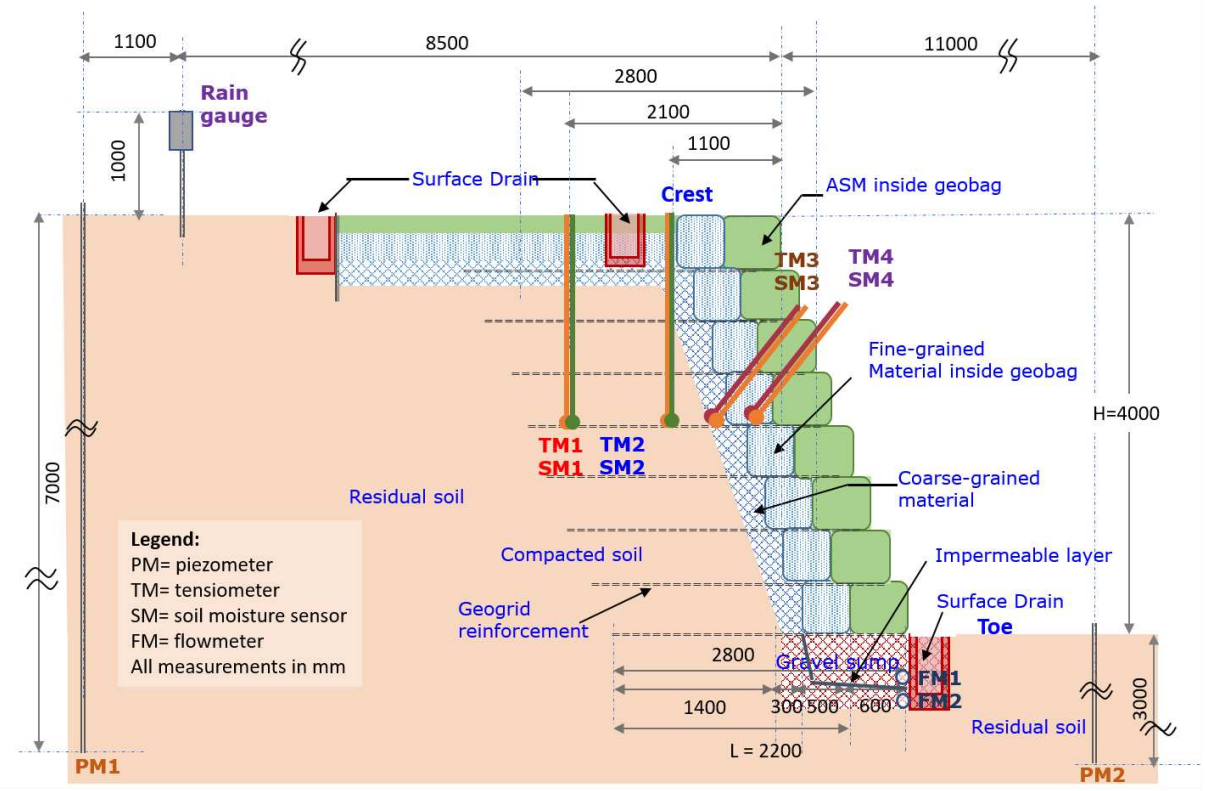


Figure 5. Cross-section of GBS at Orchard Boulevard with instrumentations.

The GBSs were instrumented to monitor their response to actual rainfall. The site was instrumented with a rain gauge to monitor rainfall and two piezometers (PM1 and PM2), located near the toe and crest respectively, to monitor groundwater table. Each GBS was instrumented with four pairs of tensiometers (TM) and soil moisture sensors (SM) to monitor pore water pressure (PWP) and volumetric water content (VWC). Two pairs of tensiometers and soil moisture sensors (TM1- SM1 and TM2-SM2) were installed vertically from the crest to monitor the pore water pressures and moisture contents of the compacted residual soils. The other two pairs of tensiometers and soil moisture sensors (TM3-SM3 and TM4-SM4) were installed perpendicular to the sloping face. These instruments measured the pore water pressure and moisture content of the coarse- and fine-grained materials, respectively. In addition, two flowmeters were installed in the gravel sump of each GBS to measure water flow from the fine-grained layer (FM1) and coarse-grained layer (FM2). The measurements by flow meters were intended to observe if there was a breakthrough from the fine-grained layer to the coarse-grained layer. The positions of all tensiometers, soil moisture sensors and flow meters in the GBSs are shown in Figure 5. All instrumentation readings were collected by a data logger at a 10-minute interval regardless of rainfall events. The data logger sends all data to a server (PC) using general packet radio service (GPRS) system over the internet. User Accounts were set up to allow all members involved in the slope project to assess the system over the internet any time, anywhere, obtaining the latest information about the slope's "health conditions". The collected data can be displaed on the webpage in time-history plots and other necessary charts for easy reference.

Material Selection for Capillary Barrier Effect

The configuration of the capillary barrier was evaluated based on several criteria. Smersud and Selker (2001) proposed that for an effective capillary barrier, the ratio of particle size (defined as d_{50}) of the coarse- and fine-grained materials should be greater than 5. Furthermore, Rahardjo et al. (2007) suggested some criteria based on: i) the water-entry value, ψ_w, of the coarse-grained soil (preferably <1 kPa); ii) the ratio between the water-entry value of the fine-grained material and the coarse-grained material (ψ_w-ratio) to be greater than 10, iii) the saturated coefficient of permeability of the fine-grained non-cohesive material (preferably $>10^{-5}$ m/s). The grain size distributions of coarse RCA and fine RCA as well as coarse RAP and fine RAP are shown in Figure 6 while the drying and wetting SWCCs of the materials are presented in Figure 7.

The required properties derived from Figure 6 and 7 for the evaluation of capillary barrier effect are summarized in Table 2. Evaluation of the properties shows that the d_{50} ratios of the coarse and fine materials of GBS1, GBS2, and GBS3 were 13, 14 and 70, respectively which were greater than 5. The ψ_w-ratio of the fine- and coarse-grained materials of GBS1, GBS2, and GBS3 were 150, 32.5 and 188, respectively, which were greater than 10. The water-entry value (ψ_w) of coarse RCA and RAP were 0.1 and 0.08 kPa which were less than 1 kPa. The coefficient of saturated permeability of fine RAP was 4×10^{-4} m/s, which was greater than 10^{-5} m/s; however, the coefficient of saturated permeability of fine RCA was 1×10^{-6} m/s, less than 10^{-5} m/s. The evaluation showed that the combinations of the fine- and coarse-grained materials used in GBS1, GBS2, and GBS3 fulfilled all the criteria except for the coefficient of saturated permeability of fine RCA. Thus, in general the combinations of fine- and coarse-grained materials used in GBSs at Orchard Boulevard were effective as capillary barrier.

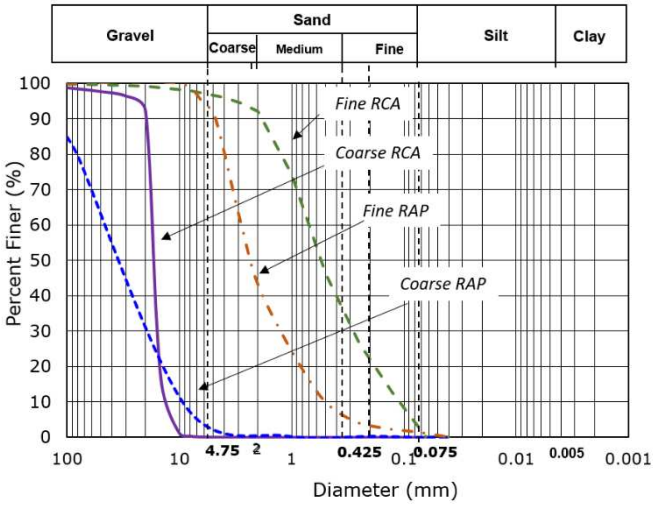


Figure 6. Grain size distribution of fine RCA, coarse RCA, fine RAP and coarse RAP.

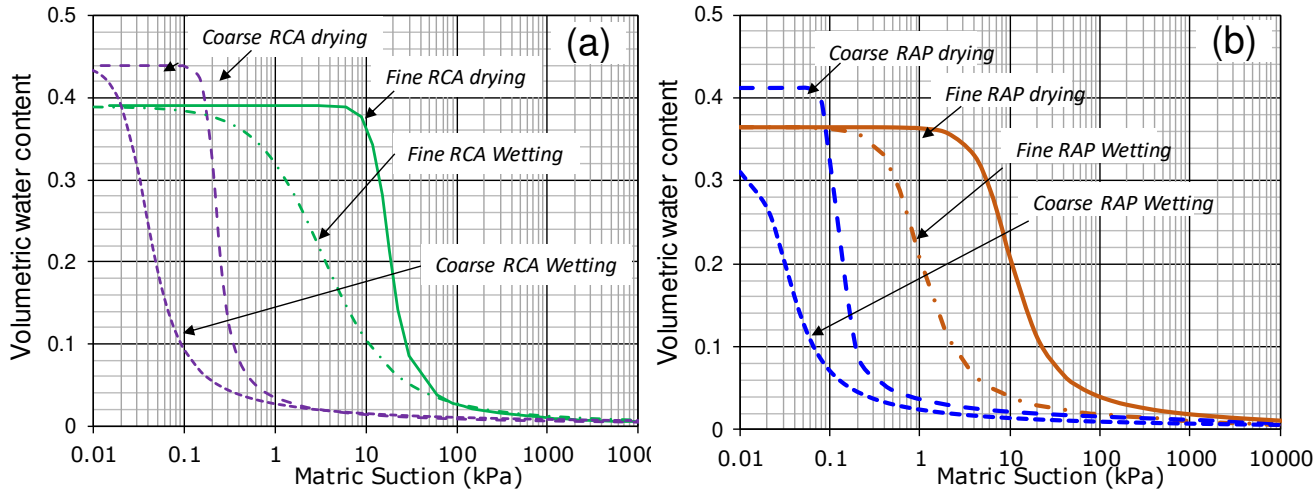


Figure 7. SWCCs of (a) fine RCA and coarse RCA and (b) fine RAP and coarse RAP.

Table 2. Evaluation of capillary barrier effect.

Parameter	Fine RCA	Coarse RCA	Fine RAP	Coarse RAP
Diameter, d_{50} (mm)	0.5	17	2.5	35
d_{50} ratio	For GBS1 = 34 ; GBS2 = 14 ; GBS3 = 70; all > 5			

Water-entry value, ψ_w (kPa)	15	0.1 (< 1)	2.6	0.08 (< 1)
ψ_w-ratio	For GBS1 = 150 ; GBS2 = 32.5; GBS3 = 188; all > 10			
Coefficient of saturated permeability k_s (m/s)	10^{-6} ($<10^{-5}$)	4×10^{-3}	4×10^{-4} ($>10^{-5}$)	1.2×10^{-3}

Field Performance

The performance of the GBSs at Orchard Boulevard was monitored for one year i.e. from 1st July 2016 to 30th June 2017. Figure 8 shows daily rainfall during the monitoring period. Rainfall monitoring at the study site indicated that the monthly rainfalls were quite different from the typical trend in Singapore. The cumulative yearly rainfall was 2819 mm which was higher than the average annual rainfall in Singapore based on the long term record from NEA Singapore (1981–2010) i.e. 2166 mm (National Environmental Agency, 2018). The number of rainfall days during the monitoring period was 178 days, which was higher than the average annual number of rainfall days in Singapore (167 days) (National Environmental Agency, 2018). The maximum daily rainfall occurred during the monsoon period in January 2017 i.e. 103.8 mm. The month of January 2017 started with a dry period for about two weeks and ended with a very wet period towards the end of the month. Therefore, rainfalls in the second half of January 2017 were selected for numerical analysis of the response of GBSs to rainfall infiltration.

Figure 9 shows the groundwater fluctuation in response to rainfall. The difference on the elevation at crest and elevation at toe (4 m) is considered in this figure. The initial groundwater table recorded by PM1 was -6.05 m with reference to the ground surface at the crest while PM2 recorded a groundwater table at -2.37 m with respect to the ground surface at the toe. The highest groundwater table during the field monitoring was -4.37 m below the ground surface at the crest (PM1) and -0.44 m below the toe. In other words, the groundwater table never rose above the ground surface during the monitoring period.

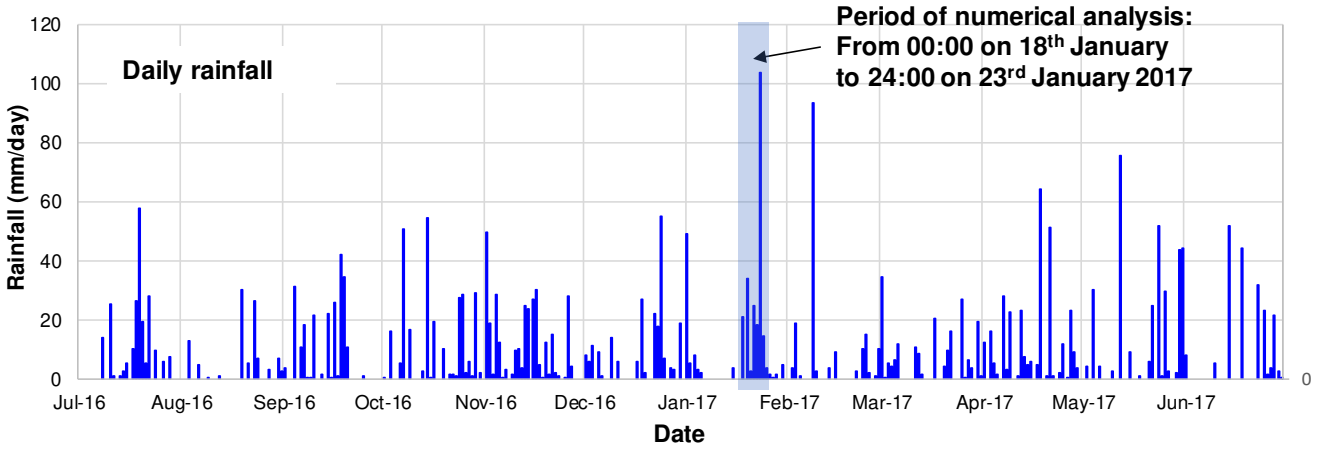


Figure 8. Daily rainfall during the monitoring period (1st July 2016 – 30th June 2017).

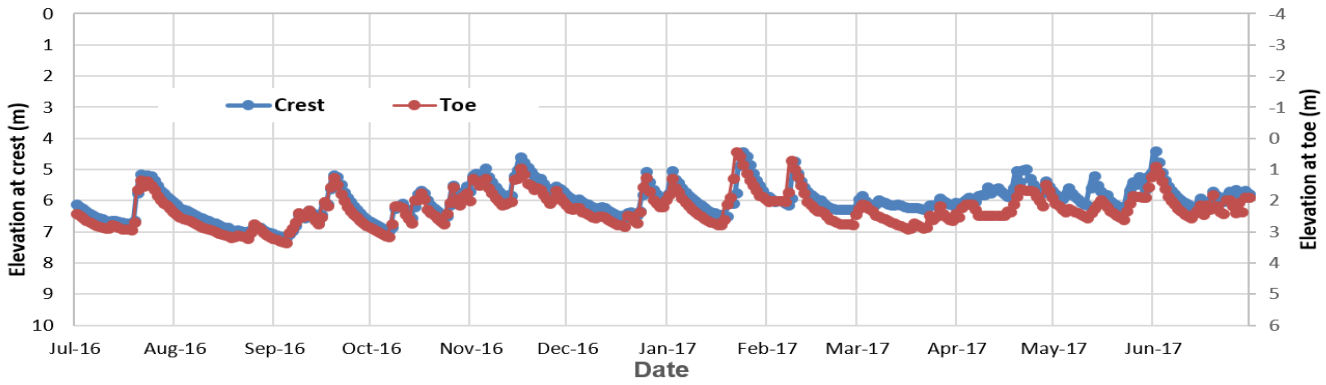


Figure 9. Groundwater table fluctuation in response to rainfall.

Transient pore water pressure (PWP) and volumetric water content (VWC) recorded by tensiometers and soil moisture sensors in GBS1, GBS2, and GBS3 during the monitoring period are presented in Figures 10 and 11. TM1 and TM2 were located in the compacted soil; however, the location of TM1 was closer to the border between the compacted residual and the original soil. Thus, the soil around TM1 was expected to be more affected by the change in the moisture content as compared to the soil around TM2. The PWP recorded by TM2 (1.1 m from slope face) in GBS 1 varied from -24 to -42 kPa whereas in GBS2 and GBS3 the PWP were almost constant at -20 kPa. The VWCs recorded by SM2 were almost constant at 40% for GBS1, 34% for GBS2 and 26% for GBS3. This could be due to the uneven compaction of the reinforced soil. PWP recorded by TM1 (2.1 m from slope face) in GBS2 only varied between 20 and 24 kPa while the variations recorded by TM1 in GBS1 and GBS3 were quite significant. During the long dry period, the PWP of TM1 could reach -86 kPa, but the reading recovered as soon as rain started to fall. The large fluctuation in PWP recorded by TM1 could be due to the effect of uneven compaction near the end of the reinforced soil zone. The corresponding VWC recorded by SM1 was between 10% and 30% in all GBSs. The PWP in coarse materials (TM3) was almost constant with time while the readings from TM4 (fine materials) fluctuated slightly between -12 and -19 kPa. Correspondingly, the VWC recorded by SM3 was constant while the VWP recorded by SM4 varied from 20% to 30% in GBS1 and from 10% to 20% in GBS2 and GBS3. Flowmeters were installed in the gravel sump to observe if there was a breakthrough from the fine-grained layer to the coarse-grained layer. The one-year monitoring shows that the flow meters did not record any flow from both the fine- and coarse-grained layers. This shows that rainwater mostly became run off or absorbed by the ASM layer.

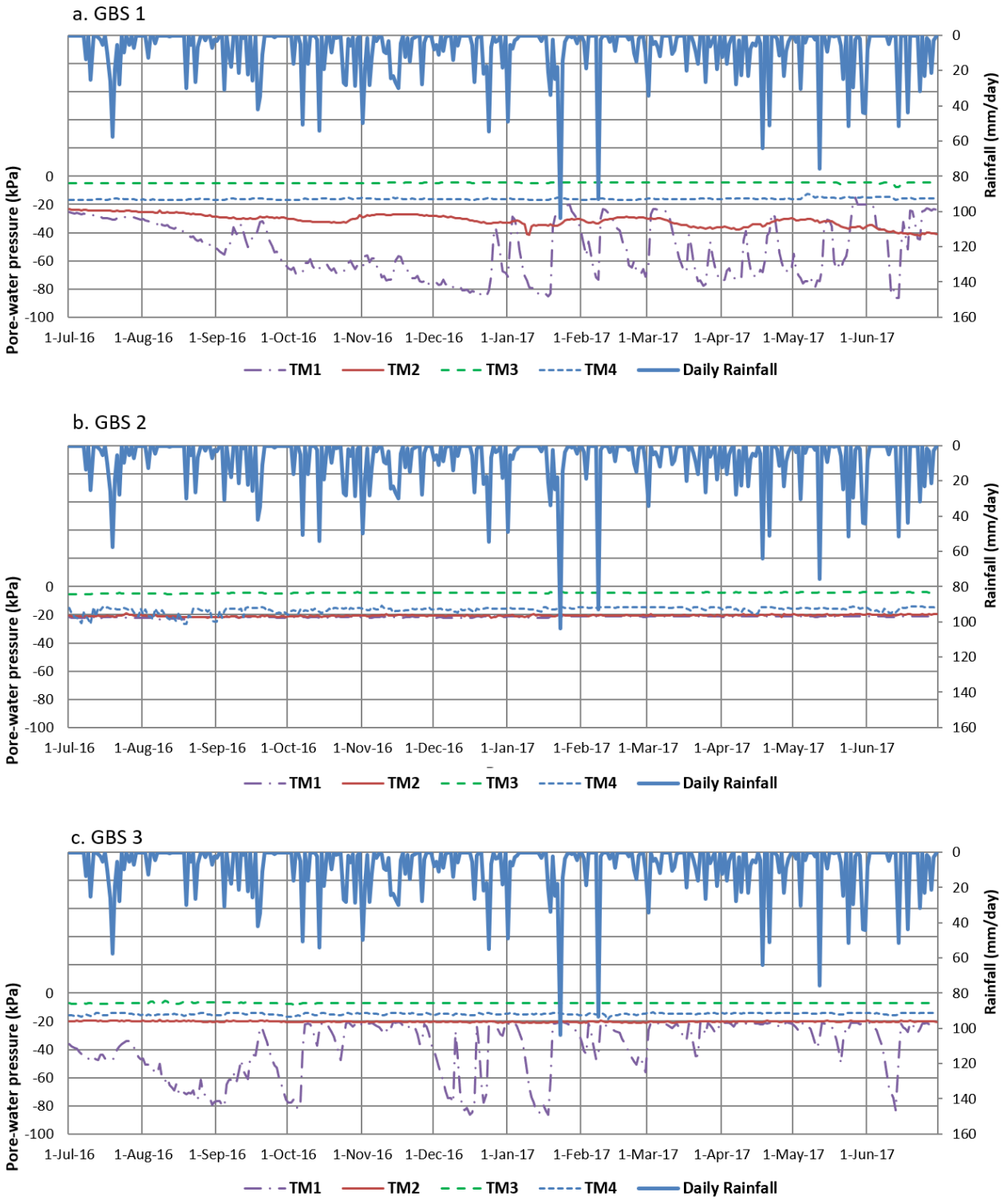


Figure 10. PWP recorded by Tensiometers in GBSs during monitoring period.

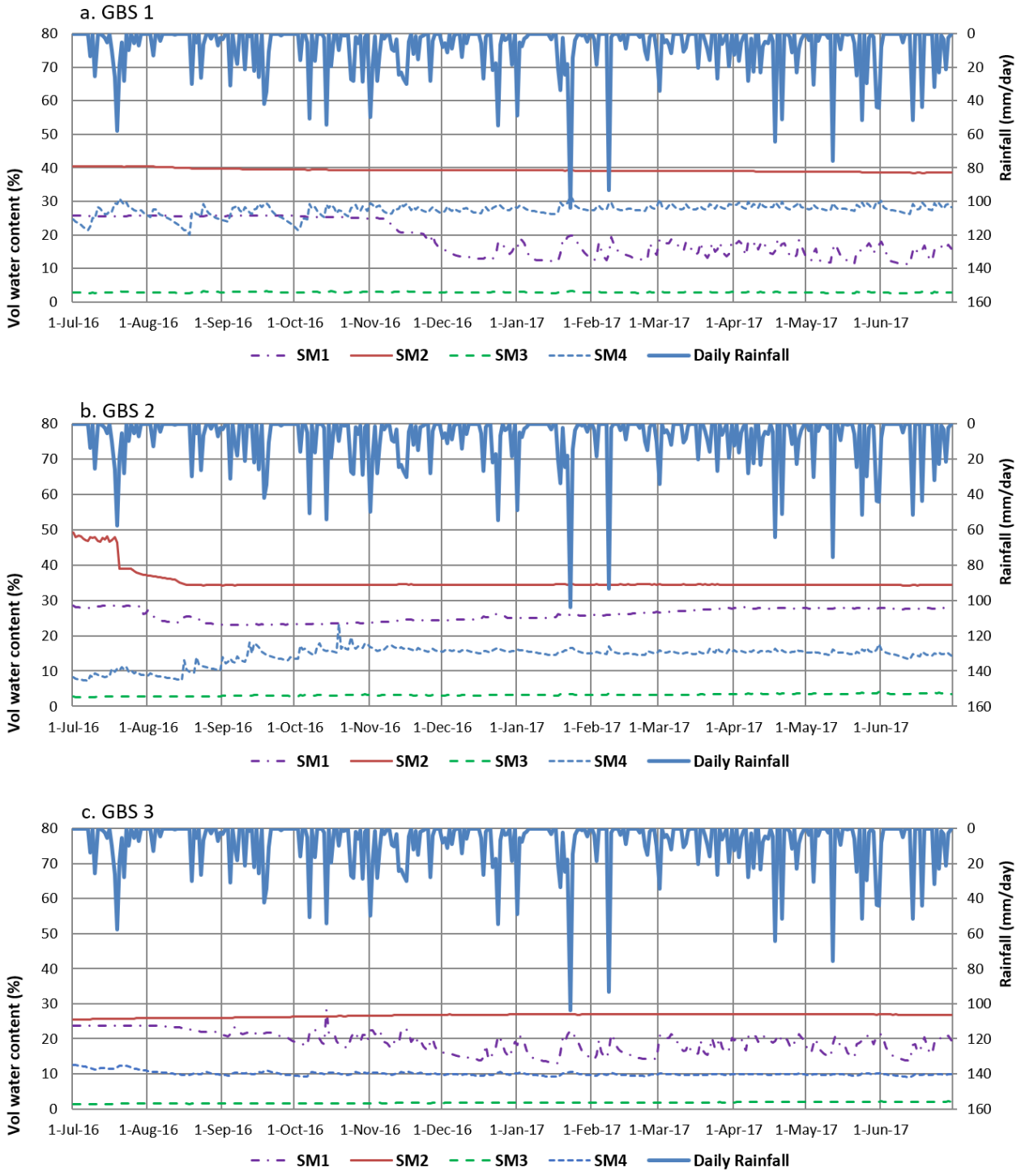


Figure 11. VWC recorded by soil moisture sensors in GBSs during monitoring period.

Numerical Analyses

Numerical analyses were carried out to study the response of GBS1, GBS2 and GBS3 in Orchard Boulevard to extreme rainfalls that occurred from 18th to 23rd January 2017 using SEEP/W program (Geoslope International, 2012a). The finite element model adopted in this study was a two-dimensional plane strain model. The boundary conditions applied to the finite element model are illustrated in Figure 12. The left and right boundaries were set at 10 m from the crest and toe of the sloping

wall, while the bottom boundary was set at 8 m from the ground surface at the toe of the slope. The mesh consisted of 3593 rectangular and triangular elements. For seepage analysis, no flow boundaries were simulated by assigning a nodal flux Q equal to zero at the bottom and both sides of the slope model above the groundwater level (GWL). A constant total head h_w was applied on each side boundary below GWL. Rainfall was applied to the ground surface as a flux boundary q. Ponding was not allowed to occur on the ground surface. This means that the pore water pressure on the ground surface was not allowed to be higher than 0 kPa. This condition simulated the actual condition whereby the excess rainwater on the slope would become surface flow or runoff. The initial pore-water pressure within the residual soil behind the GBS wall was set based on the depth of groundwater table from the ground surface while the initial pore-water pressure within the GBS was set as the pore-water pressure condition on 18th January 2017.

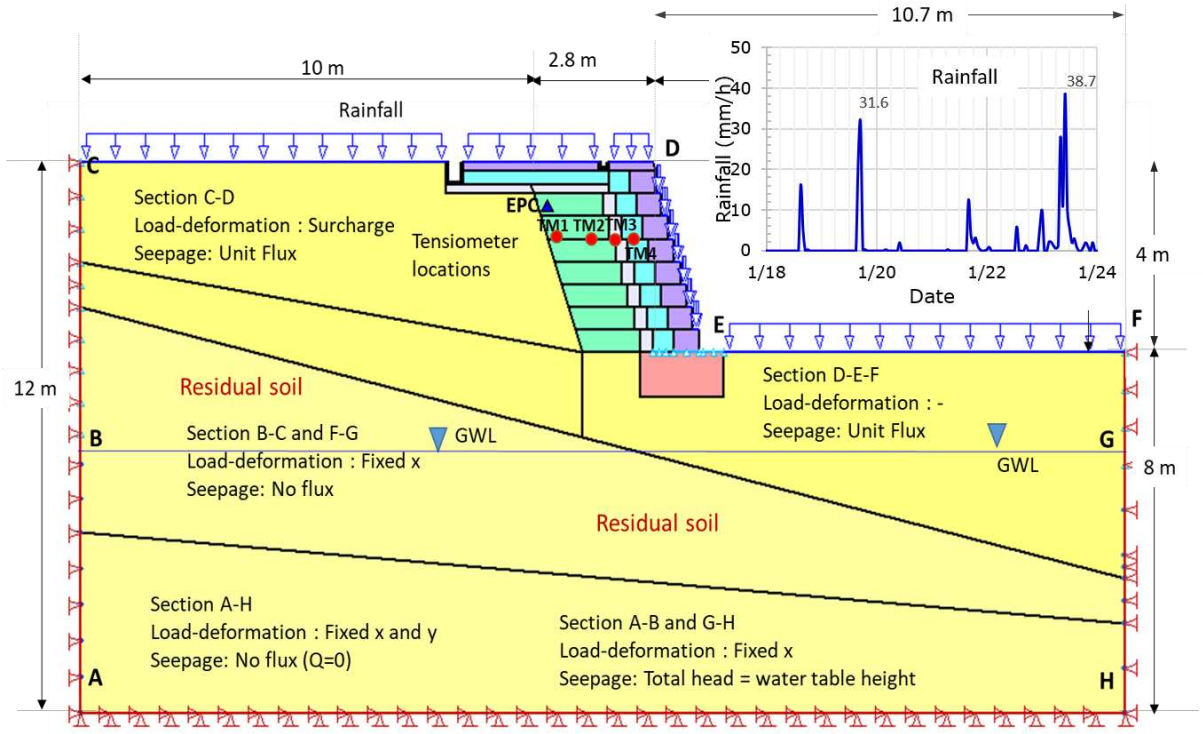


Figure 12. Finite element mesh and boundary conditions.

The drying and wetting SWCCs of the residual and compacted residual soils as well as the ASM and gravel are shown in Figure 13 while the drying and wetting SWCCs of the fine and coarse RCA as well as the fine and coarse RAP are shown in Figure 7. Wetting SWCCs were used in the numerical analysis to replicate the wetting process due to the extreme rainfall. In addition, Bashier et al. (2016) indicated that the use of wetting SWCC and permeability function is associated with worst scenario since the numerical analysis results predicted a higher infiltration rate. Hence, the factor of safety is the lowest if the numerical analysis incorporates wetting SWCC and permeability function. The wetting permeability function was determined from the SWCC wetting curves of all materials using a statistical method (Child and Collis-George, 1950) are shown in Figure 14.

Slope stability was evaluated using the SLOPE/W program (Geoslope International, 2012b) at several stages during rainfall. Bishop method was adopted in the analysis to search for the most critical slip surface within the GBS and to calculate the factor of safety. The unsaturated shear strength of materials used in the analysis is shown in Table 3.
Pore-water pressures predicted by numerical analyses at locations of TM1, TM2, TM3, and TM4 are presented in Figure 15. Spatial function was used in the numerical analyses based on PWPs recorded by the tensiometers at 00:00 on 18th January which presents the condition after two-weeks of dry period in January 2017. Thus, the recorded PWPs by TM1 in GBS1 and GBS3 were very low i.e. about -85 kPa. However, both field and numerical analyses show that the PWP responded immediately to 16.3 mm rainfall at 15:00 on 18th January even though the numerical analyses predicted a faster response to rainfall.

The fast response of soil around TM1 to rainfall (Figure 15) could be due to its position close to the border between the compacted soil and the original soil. However, the PWP became constant at about 20 kPa after rainfall. The numerical predictions of PWP at TM2 were in agreement with field data. The constant PWP shows that water did not actually seep into the compacted soil in the GBS at the location of TM2. The numerical analyses predicted lower PWP in the coarse layer (TM3) and higher PWP in fine layer (TM4) as compared to the field measurement. However, the difference was not significant.

Figure 16 shows the critical slip surface obtained from stability analyses of the slope with GBS at the end of rainfall. Since the PWP was generally constant, the factor of safety was almost constant with time. The transient FOS for all GBS is shown in Figure 17.

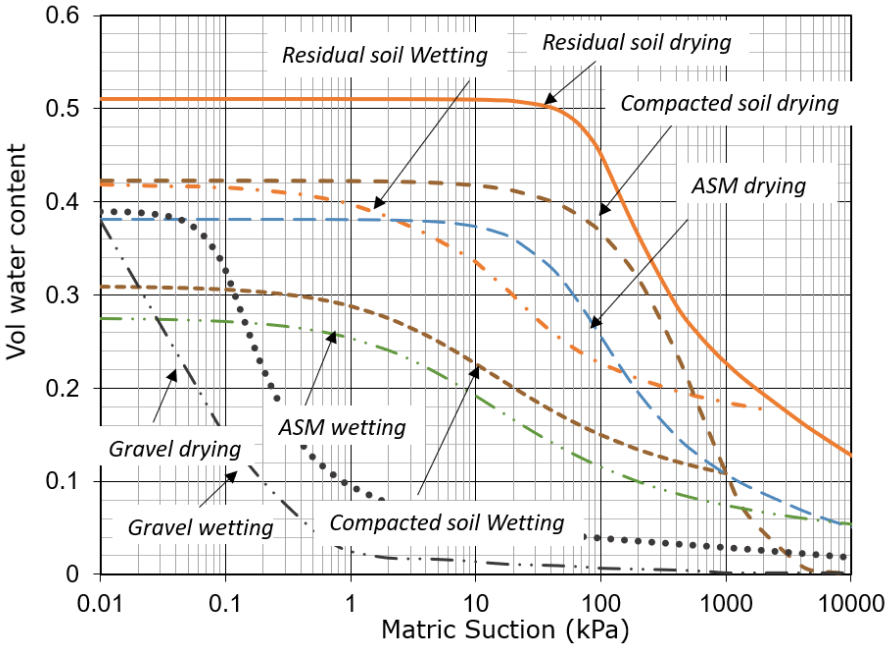


Figure 13. SWCC of Residual and compacted residual soil, and ASM and Gravel.

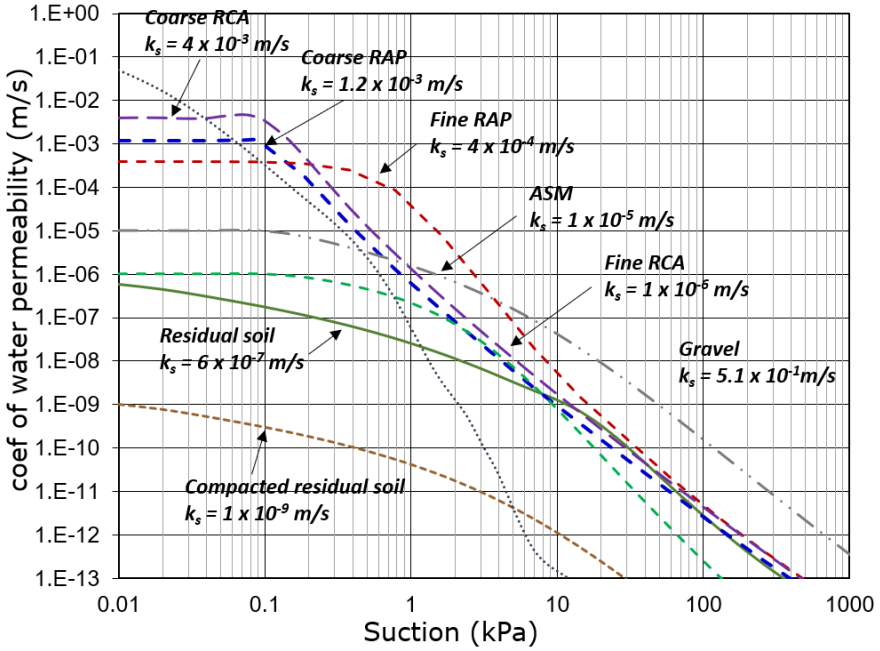
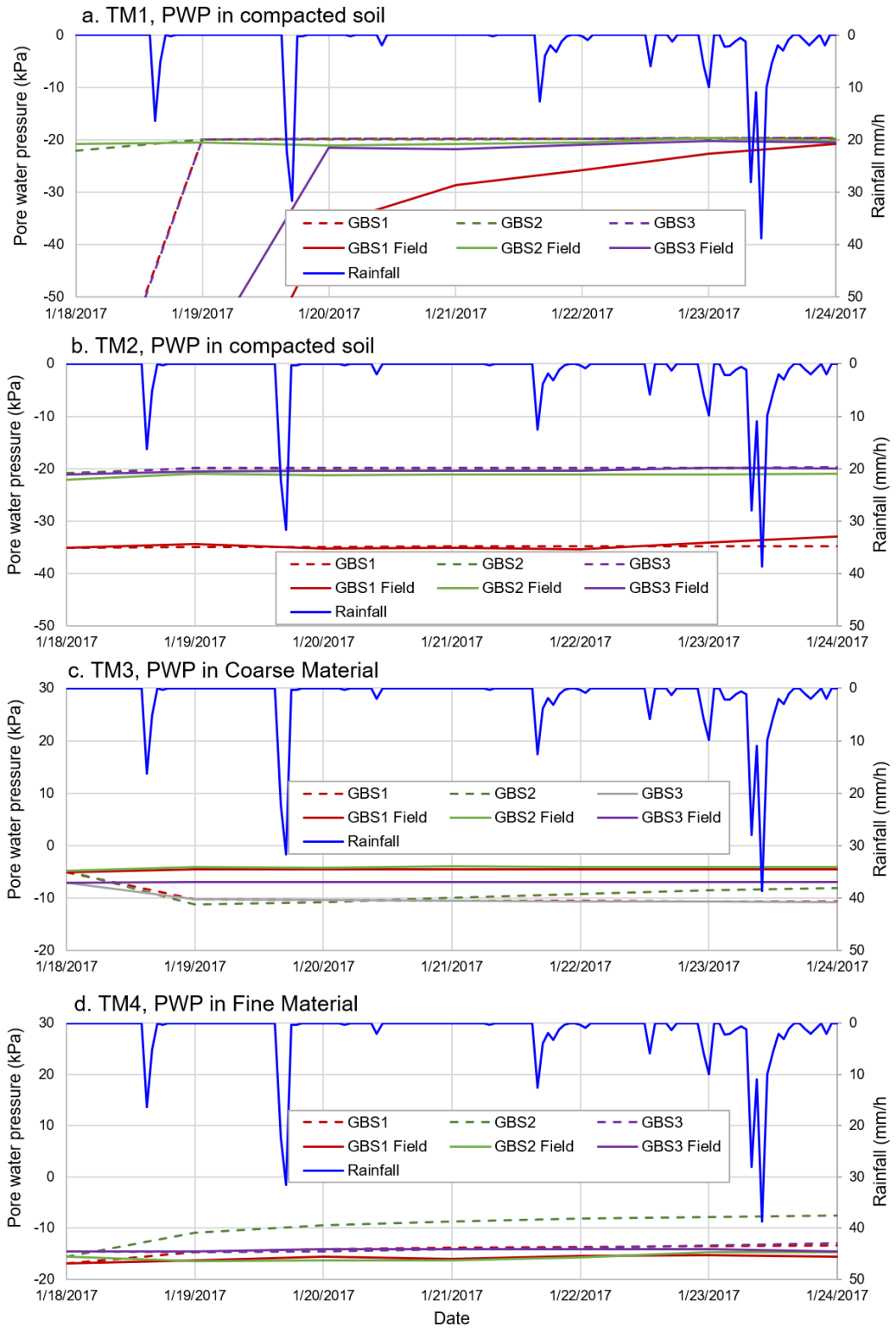


Figure 14. Permeability functions of all materials used in GBS.



Note: Field measurements = solid line
Numerical analysis results = dashed lines

Figure 15. Transient PWP predicted by seepage analysis as compared to field data.

Table 3. Unsaturated shear strength parameters for slope stability analysis.

Parameter	Effective cohesion, c' (kPa)	Effective friction angle, ϕ' (°)	ϕ^b (°)	Total unit weight, γ_b (kN/m^3)
Residual soil	5	28	17	18
Compacted residual soil	3	37	23	20
Fine RCA	0	32	15	20
Coarse RCA	0	37	17	21
Fine RAP	0	34	17	20
Coarse RAP	0	42	21	21
ASM	2	30	15	18
Gravel	0	40	-	21

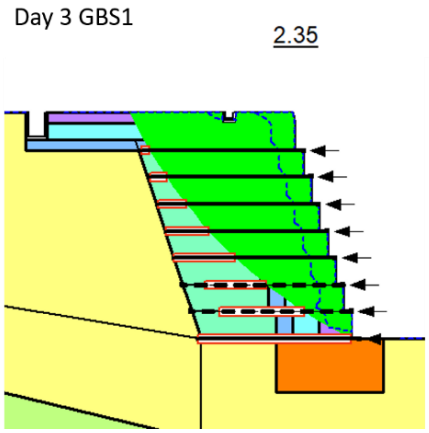


Figure 16. Critical slip surface slope stability analysis.

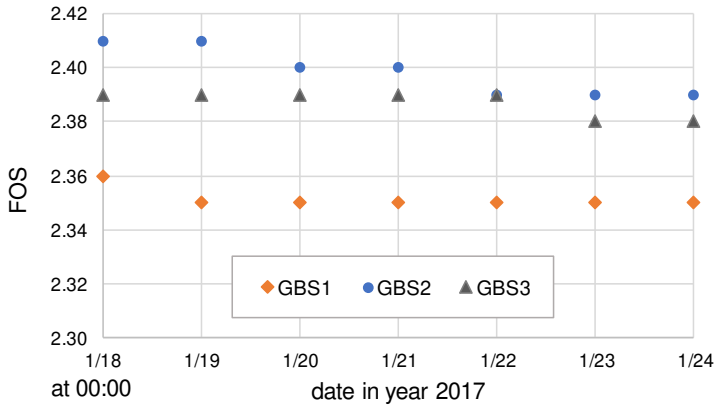


Figure 17. Transient Factor of safety predicted by slope stability analysis.

CONCLUSIONS

In this paper the suitable materials, the design and the sequence of construction of a new retaining structure incorporating capillary barrier system for preventing rainfall-induced slope failures, called Geobarrier system, have been explained in detail. Field instrumentation has shown that the GBS was effective in minimizing rainwater infiltration into the slope during rainfall. Recycled concrete aggregates and reclaimed asphalt pavement were found to be suitable and sustainable sources to be used as the fine- and coarse-grained materials of GBS.

ACKNOWLEDGEMENT

The findings published in this paper are based on the project "GeoBarrier System for Use in Underground Structure" (Grant No. SUL2013-3) that is supported by a research grant from the Ministry of National Development Research Fund on Sustainable Urban Living, Singapore, and the works are carried out and completed in collaboration between NTU and the HDB.

REFERENCES

ASTM D1556 (2015). *Standard Test Method for Density and Unit Weight of Soil in Place by Sand-Cone Method*, ASTM International, West Conshohocken, PA.

ASTM D2487 (2010). *Standard Practice for Classification of Soils for Engineering Purposes (Unified Soil Classification System)*, ASTM International, West Conshohocken, PA.

ASTM D6838 (2008). *Standard Test Methods for the Soil-Water Characteristic Curve for Desorption Using Hanging Column, Pressure Extractor, Chilled Mirror Hygrometer, or Centrifuge*, ASTM International, West Conshohocken, PA.

AASHTO (2009). *Standard Specifications for Highway Bridges*, 17th Ed., American Association of State Highway and Transportation Officials, Washington, D.C.

Bashir, R., Sharma, J. and Stefaniak, H. (2016). "Effect of Hysteresis of Soil-water Characteristic Curves on Infiltration under Different Climatic Conditions." *Canadian Geotechnical Journal*, 53, 273-284.

Bennett, M. R. and Doyle P. (1997). *Environmental Geology, Geology and The Human Environment*, John Wiley & Sons, Inc. New York.

Childs, E.C. and Collis-George, N. (1950). "The permeability of porous materials." *Proc. of the Royal Society A, Mathematical, Physical and Engineering Sciences*, 392-405.

Clancy, J.M. and Naughton, P.J. (2008). "Design of reinforced soil structures using fine grained fill types." *Proc. 1st Int. Conf. on Transportation Geotechnics*, Nottingham, UK., 427-432.

Fredlund, D.G. and Rahardjo, H. (1993). *Soil Mechanics for Unsaturated Soils*, John Wiley & Sons, Inc., New York.

Geo-Slope International Ltd. (2012a). *SEEP/W for Seepage Analysis.*

Geo-Slope International Ltd. (2012b). *SLOPE/W for Slope Stability Analysis*.

Koerner, R.M. (2005). *Designing with Geosynthetics*, 5th ed, Prentice Hall, New Jersey.

Koerner, R.M. & Koerner, G.R. (2011). "The importance of drainage control for geosynthetics reinforced mechanically stabilized earth walls." *J. Geoengineering*, 6(1), 3-13.

Matsuoka, H., Liu, S.H. and Yamaguchi, K. (2001). "Mechanical Properties of Soilbags and Their Application to Earth Reinforcement." *Proc. Int. Symp. Earth reinforcement, Fukuoka*, Japan, 587-592.

McCulloch, T., Kang, D., Shamet, R., Lee, S.J. and Nam, B.H. (2017). "Long-Term Performance of Recycled Concrete Aggregate for Subsurface Drainage." *J. Performance of Constructed Facilities*, 31(4), 47-54.

National Environment Agency, (2018). *Meteorological Services Data*.

NParks Board Singapore, (2013). *Specifications of Soil Mixture for general landscaping Use*, CUGE Publication.

Rahardjo, H., Gofar, N. Harnas, F. and Satyanaga, A. (2018a). "Effect of Geobags on Water Flow through Capillary Barrier System." *Geotechnical Engineering J. of the SEAGS & AGSSEA*, 49(4).

Rahardjo, H., Gofar, N. and Satyanaga, A. (2018b). "Performance of Geobarrier System under Rainfall Infiltration." ***Proc.*** *11th International Conference on Geosynthetics*, Seoul.

Rahardjo, H., Satyanaga, A., Harnas, F.R. and Leong, E.C. (2016). "Use of Dual Capillary Barrier as Cover System for a Sanitary Landfill in Singapore" *Indian Geotechnical J.*, 46(3), 228-238.

Rahardjo, H., Zhai, Q., Satyanaga, A., Leong, E.C., Wang, C.L., and Wong, L.H. (2015). "Geo-Barrier System as a retaining structure." *Proc. 6th AP-UNSAT2015 Conf.*, Guilin, PR China., 871-876.

Rahardjo, H., Satyanaga, A., Leong, E.C., Santoso, V.A. and Ng, Y.S. (2014). "Performance of An Instrumented Slope Covered with Shrubs and Deep Rooted Grass." *Soils and Foundations*, 54(3),417-425.

Rahardjo, H., Santoso, V.A. Leong, E.C. Ng, Y.S. Tam C.P.H. and Satyanaga, A. (2013). "Use of Recycled Crushed Concrete and Secudrain in Capillary Barrier for Slope Stabilization." *Canadian Geotechnical J.*, 50, 1-12.

Rahardjo, H., Satyanaga, A. and Leong, E.C. (2012a). "Unsaturated Soil Mechanics for Slope Stabilization." *Geotechnical Engineering J. of the SEAGS & AGSSEA*, 43(1), 48-58.

Rahardjo, H., Santoso, V.A., Leong, E.C., Ng, Y.S. and Hua, C.J. (2012b). "Performance of an Instrumented Slope Covered by a Capillary Barrier System." *ASCE J. Geotechnical and Geoenvironmental Eng.*, 138(4), 481-490.

Rahardjo, H., Santoso, V.A., Leong, E.C., Ng, Y.S. and Hua, C.J. (2011). "Numerical Analyses and Monitoring Performance of Residual Soil Slopes." *Soils and Foundations*, 51(3), 471-482.

Rahardjo, H., Krisdani, H., Leong, E.C. Ng, Y.S., Foo, M.D. and Wang, C.L. 2007. "Capillary Barrier as Slope Cover." *Proc. 10th Australia New Zealand Conf. on Geomechanics*, Brisbane, Australia, 698-703.

Rahardjo, H., Lee, T.T., Leong, E.C. and Rezaur, R.B. (2005). "Response of a Residual Soil Slope to Rainfall." *Canadian Geotechnical J.*, 42(2), 340-351.

Siah, G.C. and Tseng, C.Y. (2011). "The Major Design Considerations of Gabion Wall for Stream Bank." *Proc. of International Conference on Materials for Renewable Energy & Environment (ICMREE)*, Shanghai, China.

Smesrud, J. and Selker, J., (2001). "Effect of Soil-Particle Size Contrast on Capillary Barrier Performance." *ASCE J. Geotechnical and Geoenvironmental Eng.*, 127(10), 885-888.

Tami, D., Rahardjo, H., Leong, E.C. and Fredlund, D.G. (2004). "Design and Laboratory Verification of a Physical Model of Sloping Capillary Barrier." *Canadian Geotechnical J.*, 41(5), 814-830.

Toll, D.G., Rahardjo, H. and Leong, E.C. (1999). "Landslides in Singapore." *Proc. 2nd Int. Conf. Landslides, Slope Stability and Safety of Infra-Structures*, Singapore, 269–276.

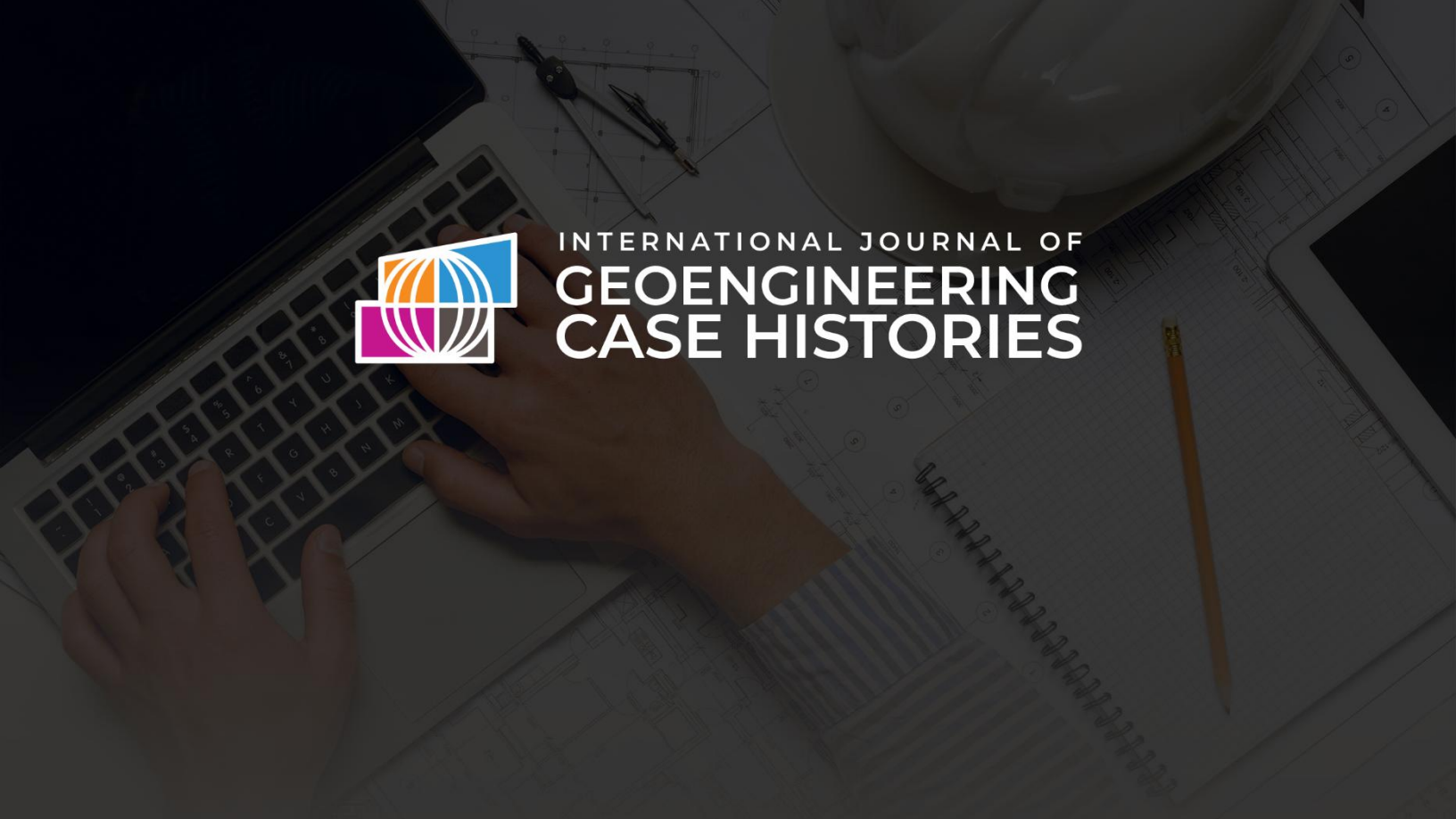
Tsaparas, I., Rahardjo, H., Toll, D.G. and Leong, E.C. (2002). "Controlling Parameters for Rainfall-Induced Landslides." *Computer and Geotechnics.*, 29(1), 1-27.

Wen, H., Wu, J.J., Zou, J.L., Luo, X., Zhang, M. and Gu, C.Z. (2016). "Model Tests on The Retaining Walls Constructed from Geobags Filled with Construction Waste." *Advances in Materials Science and Engineering*, 2016, 1-13.

Yan, S. and Chu, J. (2008). "Geobag Method for Levee Construction and Rehabilitation." *Proc. of the GeoCongress*, New Orleans, USA, 694–699.

Zhai, Q, and Rahardjo H. (2012). "Determination of soil–water characteristic curve variables." *Computer and Geotechnics*, 42, 37-43.

Zhan, TLT, Li, H, Jia, GW, Chen, YM and Fredlund, DG (2014). "Physical and numerical study of lateral diversion by three layer inclined capillary barrier covers under humid climatic conditions." *Canadian Geotechnical Journal*, 51(12), 1438-1448.



INTERNATIONAL JOURNAL OF
GEOENGINEERING
CASE HISTORIES

The Journal's Open Access Mission is generously supported by the following Organizations:

dar
a Sidara company

Geosyntec consultants
engineers | scientists | innovators

CONETEC
MUD BAY DRILLING
LANKELMA
Geotech DRILLING

ENGEO
Expect Excellence

Access the content of the ĪSSMGE Īnternational Journal of Geoengineering Case Histories at:
www.geocasehistoriesjournal.org

Downloaded: Saturday, November 14 2026, 16:11:45 UTC